ACS APPLIED NANO MATERIALS

www.acsanm.org Article

Engineered Nanoparticle Release from Personal Protective Clothing: Implications for Inhalation Exposure

Aigerim Maksot, Sadia Momtaz Sorna, Melissa Blevens, Ronald G. Reifenberger, Kimberly Hiyoto, Ellen R. Fisher, Tony Vindell, Yan Vivian Li, Matt J. Kipper, and Candace Su-Jung Tsai*

Cite This: *ACS Appl. Nano Mater.* 2022, 5, 2558–2568 Read Online

ACCESS | Metrics & More | Article Recommendations | Supporting Information

ABSTRACT: In this study, we investigated engineered nanoparticle (ENP) release associated with the contamination of personal protective clothing during the simulated motion of the human wearing the ENP-contaminated protective clothing and evaluated the relative ENP retention on the fabric. The release of airborne ENPs can contribute to inhalation exposure, which is the route of exposure of most concern to cause adverse health effects in the pulmonary system. The evaluation focuses on four popular fabric materials making the laboratory coats (cotton, polypropylene, polyester cotton blend, and Tyvek) and three types of ENPs (Al_2O_3, carbon black (CB), and carbon nanotube (CNT)). The magnitudes of particle contamination and resuspension were investigated by measuring the number concentration increase of airborne particles in sizes of 10 nm to 10 μm and the weight changes on fabric pieces. Collected aerosol particles and contaminated fabric surfaces were further characterized for understanding particle morphology, elements, agglomeration, and surface contamination status. The particle resuspension from the contaminated lab coat fabric was found to vary by the type of fabric material. Cotton fabric showed the highest level of particle resuspension for all three tested ENPs. Data were evaluated to determine the dominant forces responsible for ENP adhesion on the surface of the fabric. Tyvek fabric was determined as the best fabric for trapping Al_2O_3 and carbon black ENPs, indicating less resuspension of particles, meaning lower subsequent release, but not durable enough to wear for the long term compared with other fabrics.

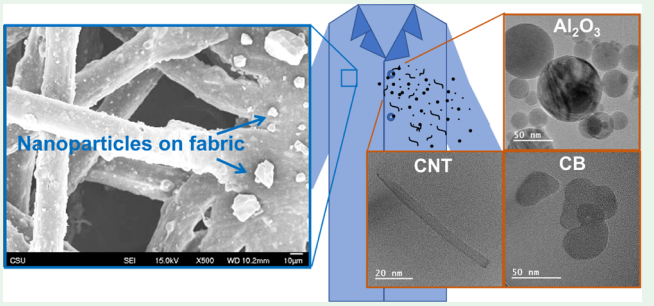

KEYWORDS: *carbon nanotube (CNT), carbon black, aluminum oxide, Tyvek, polypropylene, polyester, cotton, resuspension, lab coat*

INTRODUCTION

The nanotechnology market is expected to grow 17% annually up to 2024,[1] leading to the production of a variety of products using nanomaterials. The development of new applications with nanomaterials gives rise to risks and uncertainties regarding the exposure and adverse effects to human health and the environment.[2] One main concern with the growth of nanotechnology is the protection of frontline researchers in laboratories and workers in production facilities from exposure to engineered nanoparticles (ENPs) through inhalation or skin contact. Workers wearing contaminated clothing are at high risk of inhaling ENPs resuspended from clothing without any awareness of the potential danger. Moreover, when leaving the laboratory or production line, researchers and workers are unaware of possible ENP exposure from the contaminated clothing that they bring back to the office, home, or public places. That indicates the risk to nonworkers outside of the workplace settings. It is well-documented in previous studies that a mixture of monodisperse particles with the median sizes of 3, 5, and 10 μm has the ability to resuspend from contaminated clothing surfaces during human physical activities.[3,4] ENPs have diameters that are 3 orders of magnitude smaller, and volumes that are 10^{-9} smaller, than microparticles. Therefore, ENPs represent many times more particles than an equivalent mass or volume of microparticles resuspended from contaminated clothing.

In a pilot study, Tsai et al. studied a few commonly used fabric swatches and measured the level of nanomaterial release associated with each fabric type.[5] A substantial amount of particles were released from these contaminated fabric swatches during the constant manual manipulation of the fabric in both regular room and cleanroom settings.[5] A significant fraction of particles deposited onto clothing are subsequently resuspended into the air due to physical activities. This resuspension contributes to inhalation exposures.[4,6] Exposure to individual and small agglomerates of ENPs can evoke higher inflammation when compared with micrometer-

Received: December 7, 2021
Accepted: February 2, 2022
Published: February 11, 2022

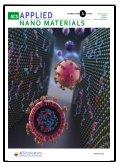

https://doi.org/10.1021/acsanm.1c04229
ACS Appl. Nano Mater. 2022, 5, 2558–2568

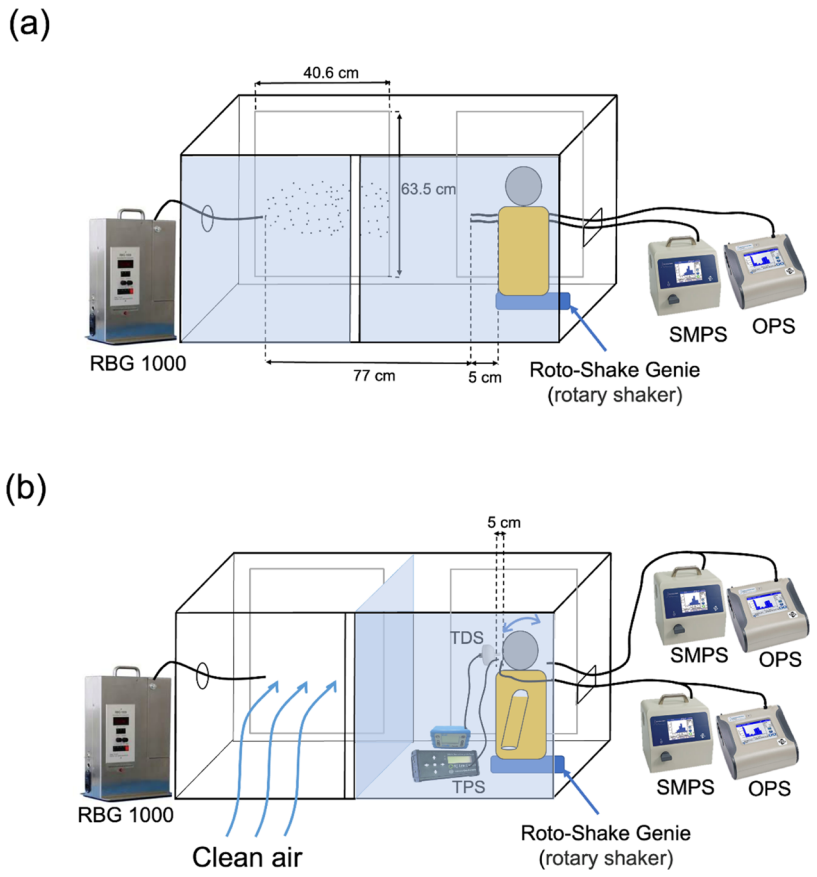

Figure 1. Illustrations of the contamination and resuspension processes and experimental setups. Clean air flew from the cleanroom toward the enclosure placed inside the fume hood. (a) Engineered nanoparticle (ENP) aerosolization for contamination on lab coats. (b) Resuspension of ENPs through shaking the mannequin and particle samplings. Note: the shaker was kept underneath the mannequin all of the time but only operated for resuspension tests.

sized agglomerates of ENPs.[7] This evidence emphasizes the importance of understanding the resuspension of nanoparticles and the status of trapping and adhesion of ENPs on the protective clothing.

To date, there are no published studies that evaluate the severity of ENP exposure associated with commonly available protective clothing fabrics or determine the affecting factors for contamination and resuspension of ENPs from the contaminated clothing. Thus, the objectives of this study are to study potential exposure contributed by human activities when wearing the ENP-contaminated personal protective clothing and quantitatively evaluate relative ENP to each fabric type. Moreover, this research aims to evaluate the primary factors responsible for ENP adhesion and release from these fabrics and identify optimal fabric characteristics for protection against toxic ENPs. With this study, workers in different fields can readily choose appropriate personal protective clothing when working with certain types of ENPs, as suggested from our results.

METHODS

This study was comprised of two evaluations that include (1) ENP potential exposure at the breathing zone associated with simulated motions of workers walking with various contaminated protective clothing and (2) qualitative evaluation regarding the characteristics attributed to ENP adhesion, retention, and resuspension from these fabrics.

Materials. The three common types of ENPs studied were multiwalled carbon nanotubes (MWCNTs), aluminum oxide (Al_2O_3), and carbon black (CB), representatives of popular ENPs in categories of high aspect ratio, hydrophilic/insulating sphere metal oxides, and hydrophobic/conducting sphere ENPs, respectively. MWCNTs are routinely produced in industrial settings by the popular chemical vapor deposition (CVD) process. The primary diameter of MWCNT (purity >95%, Nanolab, Waltham, MA) is between 10 and 30 nm, and the lengths are in micrometer ranges. Aluminum oxide (Al_2O_3) (purity 100%, Nanophase Technologies Corporation, Romeoville, IL) ENPs are spherical with an average primary size of 40 nm. Carbon black (Printex grade) is widely used in a dry powder form in printer toners and ink. The average primary size of carbon black (purity 100%, carbon black-Printex powder, Orion, Germany) is 40 nm. Four popular types of lab coat fabrics with woven vs nonwoven structures tested in this study include cotton twill woven, polyester/cotton blend (80% polyester and 20% cotton) plain woven, polypropylene spunbond nonwoven, and polyethylene spunbond nonwoven (DuPont Tyvek), respectively. All lab coats were purchased in adult size S through a commercial vendor of protective clothing. Isopropyl alcohol, distilled water, and cleanroom wipes were used to carefully clean the equipment and surfaces of the enclosure in the fume hood where experiments were performed.

Facilities, Equipment, and Procedure. The research was conducted in a class 100 level cleanroom to eliminate background aerosols and to provide the accurate measurements of ENPs. The cleanroom was operated at a slightly negative pressure, enclosed to contain particles, and exhausted to a HEPA filter with an emergency evacuation remote controller. The background particle level in this cleanroom was approximately 0−70 particles/cm^3 in the 10−420 nm size range and less than 10 particles/cm^3 in the 0.3−10 μm size range. A special enclosure was designed and placed inside the fume hood in the cleanroom to contain generated aerosols and provide a controlled

https://doi.org/10.1021/acsanm.1c04229
ACS Appl. Nano Mater. 2022, 5, 2558−2568

environment for each experiment. The enclosure was made from acrylic plastic and had two removable panels at the front to access the equipment and two filter panels (40.6 cm × 63.5 cm each) at the back to prefilter and collect airborne ENPs, which captured particles as small as 0.3 μm, before venting through the HEPA filter of the fume hood exhaust, as illustrated in Figure 1a.

RBG 1000—dust generator; SMPS—NanoScan scanning mobility particle spectrometer; OPS—optical particle sizer; TPS—thermal precipitation sampler; and TDS—Tsai diffusion sampler.

The main reason for having removable panels at the front was for access to the mannequin and equipment, and during the experiments for evaluating ENP resuspension, the left side panel was relocated to the center of the enclosure to contain the mannequin and ENP resuspension at the right side, as seen in Figure 1b.

ENPs were aerosolized by a powder dispersion generator (RBG 1000, Palas GmBH, Germany), dispersing particles with the sizes between 0.1 and 100 μm, to contaminate lab coats worn by the mannequin. When the contamination was completed, the contaminated lab coat was kept on the mannequin in the rightmost compartment of the enclosure. This compartment was further isolated with a separation panel (Figure 1b). The remaining aerosols (left side of the enclosure) outside of the isolated mannequin chamber were purged to lower the background aerosol concentration as much as possible. The separation panel was then reinserted to permit the particle resuspension measurements.

A shaker (Roto-Shake Genie rotary shaker, Scientific Industries, Bohemia, NY) was placed underneath the mannequin and held to create movement on the mannequin to simulate gentle motions of workers and the subsequent resuspension of ENPs from contaminated lab coats. The shaker was operated at 70 cycles/min with a rocking angle of 10 degrees horizontally to simulate workers' motion such as walking-related vibrations, causing particle resuspension from the contaminated lab coats.

The right and left side of the enclosure each has a hole to allow the conductive tubing of the direct reading instrument (DRI) and cables of equipment to go through (Figure 1). Particle number concentrations and size distributions of airborne ENPs during aerosolization and shaking the contaminated lab coat were measured with DRIs, including the NanoScan scanning mobility particle sizer (SMPS), a nanoparticle sizer suitable for low-concentration measurement in a cleanroom setting (TSI Model 3910, Shoreview, MN, 10–420 nm, 13 channels, concentrations 0–10^6 particles/cm^3), and the optical particle sizer (OPS) (TSI Model 3330, Shoreview, MN, 0.3–10 μm, 16 channels). The sampling flow rates for NanoScan SMPS and OPS were 0.9 and 1.0 L/min, respectively. Both DRIs when operated together measure particle concentrations for diameters from 10 nm to 10 μm with a 1 min response time. The instruments were connected with conductive tubing (Model 3001901, TSI, Shoreview, MN), which was approximately 1 m in length (i.d. of 0.48 cm) to reach the measuring locations. Mass concentrations of resuspended ENP aerosols were calculated with mass differences of sampling filters before and after particle collections, the sampling flow rates, and durations. We used a National Institute for Occupational Safety and Health (NIOSH) Manual of Analytical Methods (NMAM) 5040 to analyze the amount of elemental carbon (organic carbon and total carbon) for the collected airborne MWCNT and carbon black.[8] We also used NMAM 0500 for analyzing the mass concentration of Al_2O_3 nanoparticles and NMAM 7402 for the mass concentration of MWCNT. NMAM 7402 is typically used for the evaluation of fiber-based particles such as asbestos and recently for CNT,[9] while NMAM 0500 is used for the analysis of airborne particulates not otherwise regulated.[10] A thermal anemometer (VelociCalc 9545, TSI, Shoreview, MN) was used to measure the humidity, temperature, and air velocity to ensure all work is done in a carefully controlled environment.

Two types of nanoaerosol samplers, a Tsai diffusion sampler (TDS)[11] and a thermal precipitation sampler (TPS) (RJLee, Monroeville, Pa),[12,13] were used to collect airborne particles during the release process. The flow rate of the TDS was 0.3 L/min; it collected nano and respirable-sized particles with a cutoff aerodynamic diameter of 3.8 μm.[11] A transmission electron microscope (TEM, JEOL JEM-2100F, Peabody, MA) copper grid (SPI 200 mesh, carbon filmed) was taped onto a 25 mm diameter polycarbonate membrane filter (0.2 μm pore) and mounted in the TDS cassette. The TDS pulls air in with a sampling pump and directly collects ENPs on the grid and filter for TEM and scanning electron microscope analysis (SEM, JEOL JSM 6500 FE—SEM, Peabody, MA) to obtain morphology of ENPs. The TPS also collects ENPs directly onto a TEM grid with a flow rate of 0.05 L/min; the grids were analyzed using TEM. Due to the ferromagnetic ability, a nickel carbon-filmed TEM grid was used to sample TPS.

Experimental Process. *Aerosolization of Protective Clothing with ENPs.* ENP powders were dispersed approximately 77 cm in front of the mannequin dressed in a lab coat, which was attached with five swatches of the same lab coat fabric on the top of it to allow contamination to occur on the removable five swatches (Figure 1). A powder dispersion generator RBG 1000 was operated at a dispersing pressure of 2 bar, the piston velocity of 5 mm/h, and a rotational brush frequency of 1194 rpm. Five fabric swatches (20 cm × 20 cm) were used for each experiment, which represented the similar surface area of the lab coat where ENPs would deposit. Four fabric swatches were placed on the front side of the mannequin wearing a lab coat, and one fabric swatch was placed on the back side of the mannequin. Each swatch was weighed before and after experiments to obtain the mass changes. A set of DRIs was placed in front of the mannequin wearing protective clothing to measure the total number concentrations of exposed ENPs. According to published data regarding occupational exposure concentrations of metal-oxide particles, they were typically in the range of 10^4–10^5 particles/cm^3, including background particles.[14−19] Thus, we dispersed ENP aerosols with concentrations ranging from 10^4 to 10^5 particles/cm^3 to simulate the practical contamination of a person wearing a lab coat in such a workplace. Background concentration measurements were taken for 10 min before the experiment to determine a clear baseline to compare the concentration increase during the contamination and resuspension processes.

Resuspension of Particles from Contaminated Clothing. After surface contamination on the lab coat, the contaminated lab coat on the mannequin was then subsequently measured the suspension of ENPs, as shown in Figure 1b. Two sets of DRIs were used, one set to measure at the mannequin's nose and the other set to measure at 10–15 cm horizontally away from the back of the head, representing the breathing zone and bystander particle exposure. TDS and TPS collected particles during the release process at the same locations as DRIs at the front of the mannequin. The contaminated fabric swatches attached to the mannequin were shaken by the motion of the mannequin sitting on an automatic shaker to simulate a typical worker's motion. No air exchange occurred during this resuspension of ENPs. The ENPs deposited on the fabric surface were resuspended into the air through shaking. DRIs monitored concentrations of the whole process "at the breathing zone of the mannequin representing the particle release from the fabric to be inhaled by a worker" including background before contamination, during contamination, postcontamination, during resuspension, and postresuspension. The weight of the fabric swatches was measured before the aerosolization of ENP and after the resuspension process to evaluate the amount of ENPs trapped on the fabric swatches.

At the end of each experiment, fabric swatches were stored in a sealed bag then disposed of as hazardous waste. All surfaces were cleaned using distilled water and alcohol following standard cleanroom cleaning procedures to ensure no cross-contamination and overall safety.

Fabric descriptive property measurements and airborne particle sampling using standard methods are described in the Supporting Information (SI).

Electron Microscopy Analysis. Fabric samples, plain and contaminated, were analyzed using SEM. For SEM analysis, the sample piece was held on a substrate with carbon tape, coated with different thicknesses of gold alloy and imaged with different accelerating voltages due to the thickness of each type of fabric.

https://doi.org/10.1021/acsanm.1c04229
ACS Appl. Nano Mater. 2022, 5, 2558−2568

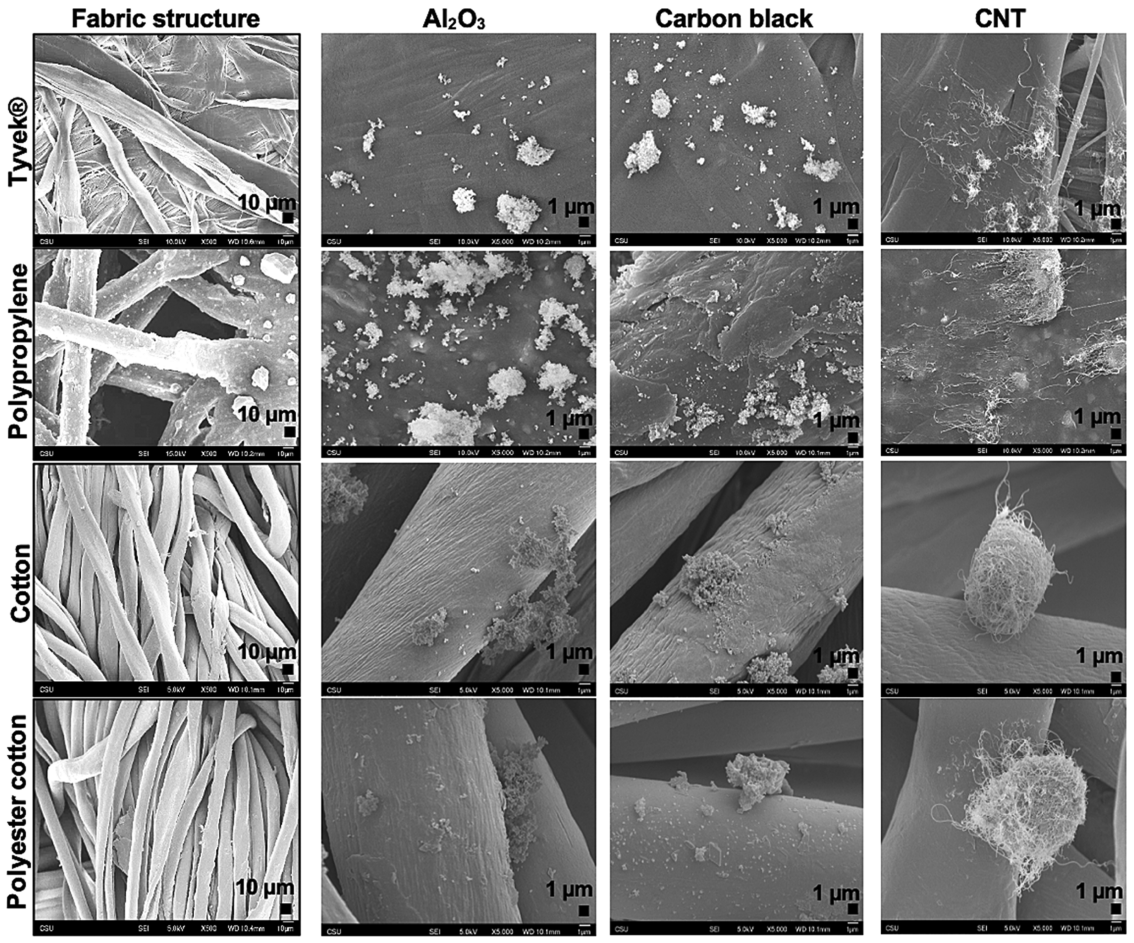

Figure 2. SEM images of the structure of each type of fabric and surface of the fabrics contaminated with three types of ENPs.

Tyvek and polypropylene samples were coated with 25 nm of gold at 10 kV and cotton and polyester cotton samples were coated with 50 nm at 5 kV for high-resolution images. Similar specifications were used for TEM analysis.

Statistical Analysis. The airborne concentrations of ENP contamination and resuspension were further analyzed to interpret the statistical significances. Statistical analysis was conducted with the R and RStudio software package (version 1.4.1106, BCorps, Boston, MA). The aerosolized particle number concentration of different ENPs and release of ENPs from different fabrics were assessed and evaluated for correlation analysis. The mass change per unit mass of contaminated fabric swatches was assessed and evaluated using standard ANOVA techniques followed by Tukey's honestly significant difference test. At a 95% confidence level, p-values <0.05 were considered statistically significant.

RESULTS AND DISCUSSION

Resuspension Status of Nanoparticles from Contaminated Clothing. According to the contamination levels of each ENP studied, the average normalized number concentration of ENPs produced by the powder dispersion generator RBG 1000 was measured in size ranges between 10 and 420 nm by Nanoscan SMPS and 0.3−10 μm OPS. Measurements were repeated three times. The average measured normalized distribution for each of three ENPs is plotted in Figure S1, and data are further described in the SI. The fabric structure and the contaminated fabric are illustrated in Figure 2. Small individuals and large agglomerates of particles were scattered across the surface of the fabric. Various morphologies of particle contaminate were observed on all types of fabric fibers.

To minimize risks of secondary exposure through contaminated clothing, it was important to determine the level of ENPs resuspension and identify the fabric that would release the least ENPs after contamination. Furthermore, any size-dependent adhesion of ENPs to a given fabric would be revealed by comparing the size distributions of resuspended particles to the generated ENPs, which contaminated the fabric. If the released distribution of ENPs was proportional to the contamination distribution, then the ENP size does not play a significant role in adhesion. If the size distribution of the released nanoparticles is significantly different from the size distribution of the generated ENPs, this might indicate that the fabric preferentially traps and/or releases ENPs as a function of size, implying a size-dependent adhesion mechanism that depends on the interaction between the ENPs and fabrics.

To investigate these questions further, the number concentration of airborne particles released from the contaminated protective clothing for each type of ENPs was measured by shaking the fabric after the contamination process. Two studies were analyzed. The first was a gravimetric study in which five fabric swatches attached to the lab coat worn by the mannequin, initially contaminated by a specific ENP (Al_2O_3, carbon black, or CNTs), were weighed on a balance to determine its mass m_o, then shaken and reweighed to measure its mass m after shaking. The fractional mass change $\Delta m/m_o$ ($\Delta m = m_o - m$) was then calculated. In the second study, the size distribution of the ENPs released by the shaking of the mannequin attached with five contaminated

https://doi.org/10.1021/acsanm.1c04229
ACS Appl. Nano Mater. 2022, 5, 2558−2568

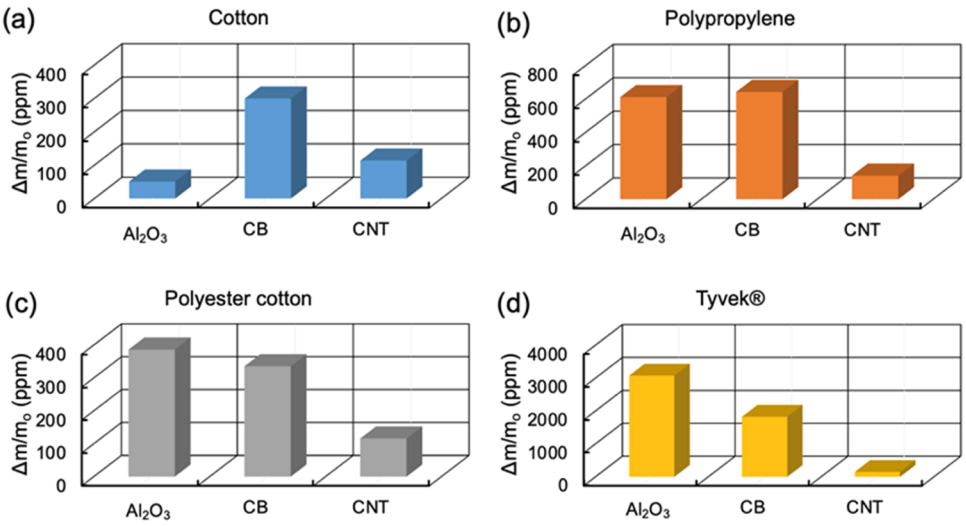

Figure 3. Fractional mass change after contamination and release of different ENPs from the four fabrics studied: (a) cotton, (b) polypropylene, (c) polyester cotton, and (d) Tyvek.

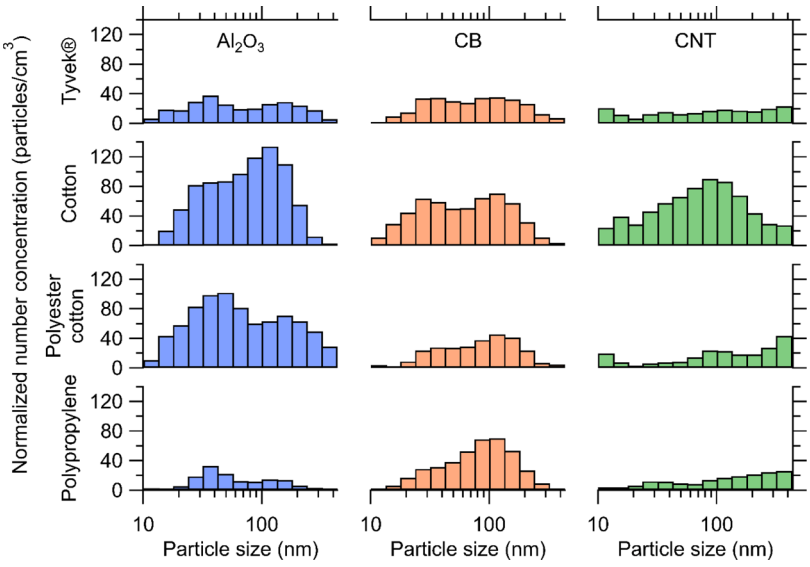

Figure 4. Measured normalized particle concentrations released after the shaking of contaminated lab coats made from Tyvek, cotton, polypropylene, and polyester cotton. Graph columns present (a) for Al_2O_3 release, (b) for carbon black (CB), and (c) for carbon nanotube (CNT).

fabric swatches was then determined for each of the fabrics under study using the DRI instrumentation shown in Figure 1. This analysis allowed a detailed size distribution of the released ENPs to be determined. Using these two analyses provided an estimate for the ENPs released by shaking, the amount of ENPs retained on the fabric and an integrated snapshot of the released ENPs irrespective of ENP size.

Mass Change Analysis. The mass change of a fabric swatch after shaking is a straightforward way to measure the extent that ENPs of different types adhere to each fabric. Because the thickness of each fabric type studied is different, it is difficult to directly compare the fractional mass change of a given ENP between fabrics. Instead, the gravimetric data are most useful to assess the trends between the different types of ENPs released by one fabric. The mass change data per unit mass of fabric are provided in Figure 3.

According to Figure 3, Tyvek fabric showed the highest mass change per unit mass from the Al_2O_3 ENP contamination (3078 ppm), while polypropylene, polyester cotton, and cotton presented lower mass change per unit mass of 611.6, 386.3, and 50.6 ppm, respectively. Cotton and polyester cotton fabric were much thicker with higher weight m_o than Tyvek and polypropylene, resulting a lower mass change per unit mass of fabric. From the contamination and release of carbon black ENPs, Tyvek was also found to be the fabric with the highest mass increase per unit mass with the value of 1821.2 ppm, followed by polypropylene with 642.1 ppm, polyester cotton with 335.5 ppm, and cotton with 299.6 ppm of mass increase per unit mass. However, the mass change per unit mass of CNT ENPs was similar for all fabrics.

Based on statistical analysis shown in Figure S2a in the Supporting Material, there is a significant difference between the mass change per unit mass of Tyvek compared with polypropylene, cotton, and polyester cotton ($p < 0.05$) with 95% confidence level. However, cotton, polyester cotton, and polypropylene are not significantly different from each other ($p > 0.05$). Figure S2b shows similar results for the mass change per unit mass from the contamination and release of carbon

https://doi.org/10.1021/acsanm.1c04229
ACS Appl. Nano Mater. 2022, 5, 2558−2568

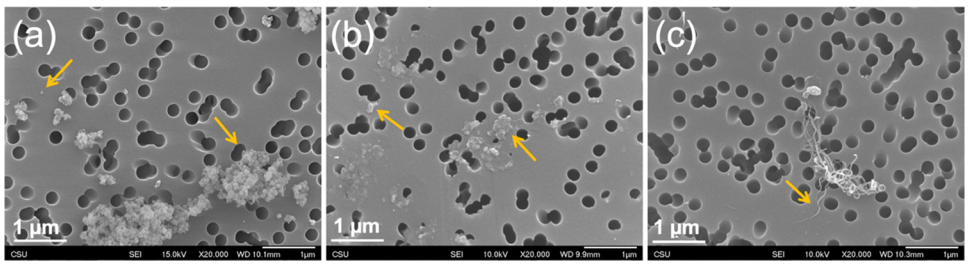

Figure 5. SEM images of resuspended ENPs collected on a polycarbonate membrane filter (0.2 μm pore) of TDS samples: (a) Al_2O_3, (b) carbon black, and (c) CNT. Arrow marks note single ENPs or agglomerates.

black ENPs. The results are quite similar to the results from Al_2O_3 (Figure S1a). The main difference the mass change per unit mass of Tyvek fabric is not significantly different from the mass change per unit mass of polypropylene fabric ($p > 0.05$). It is clearly seen from Figure S2c that there is no significant difference between fabrics from CNT ENP contamination and release tests.

Size Distribution Analysis of Released Nanoparticles. The number concentrations of released airborne particles from contaminated protective clothing for each type of ENPs are presented in Figure 4. It is significant that the concentrations of the released nanoparticles in the 10−100 nm size range are about a factor of 1000 less than the contaminating concentrations plotted in Figure 2, indicating the high degree of nanoparticle adhesion to all of the fabrics studied. Consistently for all studied ENPs, the cotton fabric showed the highest level of particle release compared with other fabric types. The highest number concentration of Al_2O_3 ENPs released from cotton fabric were 134 particles/cm^3 at a particle size of 115 nm, whereas polypropylene fabric released the least number of particles, with number concentrations less than 33 particles/cm^3. The highest number concentrations of airborne Al_2O_3 ENPs released from polyester cotton fabric and Tyvek fabric were 101 and 37 particles/cm^3 at sizes 48 and 37 nm, respectively. According to Figure 4b, the number concentrations associated with carbon black ENP release from cotton and polyester cotton fabric were lower compared with Al_2O_3 ENP release. Figure 4c shows that Tyvek, polypropylene, and polyester cotton fabric materials showed approximately similar levels of CNT ENP release concentration during manipulation; the cotton fabric released the most, followed by the Tyvek, polyester cotton, and polypropylene fabric based on the average release concentrations.

Three important conclusions can be drawn that (1) a higher release of Al_2O_3 ENPs was from cotton and polyester cotton fabrics compared to the release of either carbon black or CNT ENPs from the same fabric, (2) cotton fabric was distinctive because it showed an increased concentration of released Al_2O_3 and CNT ENPs when compared to the other fabrics studied, and (3) the release of Al_2O_3 and carbon black ENPs from all fabrics appears to have a bimodal distribution that is apparently a different size distribution, which is not related to the contaminating distribution plotted in Figure 2. This result is especially pronounced for cotton fabric, indicating that Al_2O_3 and carbon black ENPs contaminating cotton likely have a size-dependent adhesive character.

By comparing the normalized distributions in Figure 4a−c, it is clear that the release concentrations of cotton and polyester cotton in Figure 4a have a higher concentration of released Al_2O_3 ENPs when compared to released carbon black and CNTs found in Figure 4b,c. This result can be understood by the higher concentration of contaminating Al_2O_3 ENPs, as shown in Figure 2. In addition, from Figure 4a, the cotton fabric released the highest level of Al_2O_3 ENPs of all fabrics studied. This would suggest that when dealing with metal-oxide ENPs, a polypropylene and Tyvek fabric would offer clear advantages in trapping the ENPs over cotton, polyester cotton, or polypropylene fabrics.

For the case of carbon black contamination, Figure 4b indicates that the overall concentration associated with carbon black release from cotton and polyester cotton fabric was about a factor of 1.5 lower when compared with Al_2O_3 ENP release, even though Figure 2 indicates that the contaminating concentration of carbon black is comparable to that for Al_2O_3. Polypropylene and Tyvek were found to have the lowest carbon black ENP release. The data in Figure 4b further suggests a bimodal distribution of carbon black ENP release from all fabrics studied, a trend that is most clearly evident for the cotton fabric. The measured released distributions are distinctly different in shape from the contamination distribution, as shown in Figure 2, indicating that 60−70 nm sized carbon black ENPs adhere more strongly to cotton fabric than either smaller or larger sizes.

For the case of CNT contamination, Figure 4c shows that Tyvek, polypropylene, and polyester cotton fabric showed approximately similar levels of CNT ENP release during manipulation. The release concentration of CNT ENPs for cotton was the highest when compared to Tyvek, polypropylene, or the polyester cotton fabric. These levels of resuspension were associated with short-term contamination and release time. When a prolonged contamination and exposure occurs, the risk of affecting human health will increase with further results presented in this study.

The mean differences in particle release concentration were found to be statistically significant at the $p = 0.05$ level. According to Table S2, the Al_2O_3 total number concentrations resuspended from the cotton and polyester cotton fabrics were found to be significantly different from Tyvek and polypropylene, while cotton is not significantly different from polyester cotton with the p-value of 0.80. Similar to carbon black total number concentrations, cotton and polyester cotton fabrics were significantly different from Tyvek and polypropylene; however, based on the total number concentration results of CNT ENPs, cotton was turn out to be significantly different from all other fabrics at the $p = 0.05$ level. Statistical analysis on correlation was made on the resuspension concentrations of Al_2O_3, carbon black, and CNT ENPs. Based on Tables S3 and S4 from the Supplementary Material, the strong correlation between the fabrics can be observed for particle size distributions of resuspended Al_2O_3 and carbon

https://doi.org/10.1021/acsanm.1c04229
ACS Appl. Nano Mater. 2022, 5, 2558−2568

Table 1. Released Level of Airborne ENP Number and Mass Concentrations of Various Types of Lab Coat

ENPs	lab coat fabric type	at front[d] (30 min)	at back[d] (30 min)	at front[e] (6 h)	at front (6 h)	at front total carbon[f]	
		number conc. 10–420 nm (particles/cm^3)			Mass conc. (μg/m^3)	μg/sample	μg/m^3
Al_2O_3	cotton	174 ± 64	30 ± 7	258	29.8[a] ± 0.1		
	polypropylene	83 ± 41	61 ± 41	73	1.2[a] ± 0.1		
	polyester cotton	163 ± 46	101 ± 54	210	21.3[a] ± 0.2		
	Tyvek	88 ± 37	45 ± 22	75	2.2[a] ± 0.4		
Carbon Black	cotton	96 ± 21	91 ± 22	198	89.9[b] ± 0.3	20[c]	27[c]
	polypropylene	74 ± 13	69 ± 16	121	10.8[b] ± 0.1	12[c]	16[c]
	polyester cotton	102 ± 17	86 ± 19	254	79.4[b] ± 0.1	16[c]	22[c]
	Tyvek	90 ± 36	61 ± 5	114	22.2[b] ± 0.1	19[c]	27[c]
CNT	cotton	126 ± 58	108 ± 47	223	12.3[b] ± 2.4	16[c]	23[c]
	polypropylene	52 ± 15	42 ± 12	72	7.8[b] ± 4.5	13[c]	18[c]
	polyester cotton	59 ± 7	37 ± 7	105	10.8[b] ± 2.5	16[c]	22[c]
	Tyvek	42 ± 6	32 ± 23	87	2.9[b] ± 1.3	12[c]	17[c]

[a]Mass concentration calculated using NIOSH Manual Analytical Method (NMAM) 0500 close face for collecting airborne particles for 6 h at a flow rate of 2 L/min. [b]Mass concentration calculated using NMAM 7402 open face for collecting airborne particles for 6 h at a flow rate of 2 L/min. [c]Mass concentration measured using elemental carbon analysis for 6 h at a flow rate of 2 L/min. [d]Data are the average of three experiments. Each experiment has 30 sets of data. [e]Data are the average from one experiment with 360 sets of data. [f]Released total carbon is the sum of released elemental carbon and organic carbon, analyzed using NMAM 5040 collecting for 6 h.

black ENPs with low *p*-values, meaning that there is a strong relationship between the particle size distribution of manipulated fabrics. According to Table S5 related to the results of particle size distributions of released CNT ENPs, the negative or low correlation factor and high *p*-values can be seen from the comparison between the cotton and other fabrics, which indicate that there is no significant relationship between the variables.

Integrated Analysis of Released Particle Sizes, Morphology, and Concentrations. The resuspended particles collected on the polycarbonate filters of TDS samples are presented with SEM images in Figure 5. Large agglomerates and individual particles of Al_2O_3, with many smaller than 1 μm, were released from the surface of Tyvek fabric, as shown in Figure 5a. Limited amounts of carbon black particles were seen with some individual particles at approximately 50 nm (Figure 5b). As seen in Figure 5c, small CNT clusters containing single fibers were collected during the release process of Tyvek fabric. The limited amount of CNT ENPs collected implies a low resuspension concentration during the shaking process, whereas the larger amount of Al_2O_3 ENPs and carbon black released from the surface of the fabric was consistent with the higher total number concentration of released particles presented in Figure 4.

Data presenting airborne particle mass concentrations by filter-based sampling and the total number concentrations from Figure 4 are listed in Table 1 for comparisons. Based on the released total number concentrations measured by SMPS, where it is clearly seen that the release concentration measured from the front side of the mannequin was higher than the release concentration measured at the back of the mannequin. Based on the total number concentrations at the front and back sides of the mannequin, the highest release concentration of Al_2O_3 and CNT ENPs was found from manipulating cotton fabric, while polyester cotton fabric release concentration was the highest for carbon black ENPs. The total number concentration during the release of Al_2O_3, carbon black, and CNT ENPs for Tyvek and polypropylene fabrics was found to be the lowest.

Two major conclusions can be made from Table 1. First of all, the level of generated CNT aerosols was lower compared with Al_2O_3, which was an affecting factor showing a lower mass increase for all fabrics exposed with CNT ENPs. Since our focus was evaluating the difference between fabric types with the same ENP, the small variation in the generated ENP concentrations could be neglected. Moreover, CNT ENPs are considered the lightest nanoparticles among the other used ENPs; therefore, the mass increase for each type of fabric was lower compared with Al_2O_3 and carbon black ENP data. Based on these results, Tyvek is the best fabric for trapping Al_2O_3 and carbon black ENPs, resulting in less resuspension of particles from the contaminated lab coat. There is not much difference in trapping ENPs between polypropylene, polyester cotton, and cotton fabrics. Second, the difference in resuspended total number concentrations between the front and back of the mannequin, as was expected the concentrations of released particles at the breathing zone (front side) are higher than those of particles released from the back side of the worker wearing the contaminated protective clothing.

Table 1 also presents the results for the long-term exposure of released nanoparticles, with 1 h of exposure followed by 6 h of shaking. The 6 h shaking represents the time when workers wear contaminated clothing/lab coat performing gentle motion of task such as walking, moving arms siting in an office, or operating equipment during a work shift. The measurements were taken at the breathing zone presenting the particle release to be inhaled by a worker; it would have minimal effects by the room size. It is clearly seen that the release number concentration level after 1 h of exposure was much higher than the concentration after 30 min of exposure. The total number concentration during 6 h of release from the manipulation of cotton and polyester cotton fabric was around 2 times higher than 30 min of release, while there was a small difference between the 6 h and 30 min of the release of Tyvek and polypropylene.

Table 1 also presents the mass concentrations of released airborne particles following the NMAM 0500 protocol for collecting Al_2O_3 ENPs and the NMAM 7402 and 5040 protocols for carbon black and CNT ENPs. Note that a large amount of carbon black and CNT ENPs was collected because

https://doi.org/10.1021/acsanm.1c04229
ACS Appl. Nano Mater. 2022, 5, 2558−2568

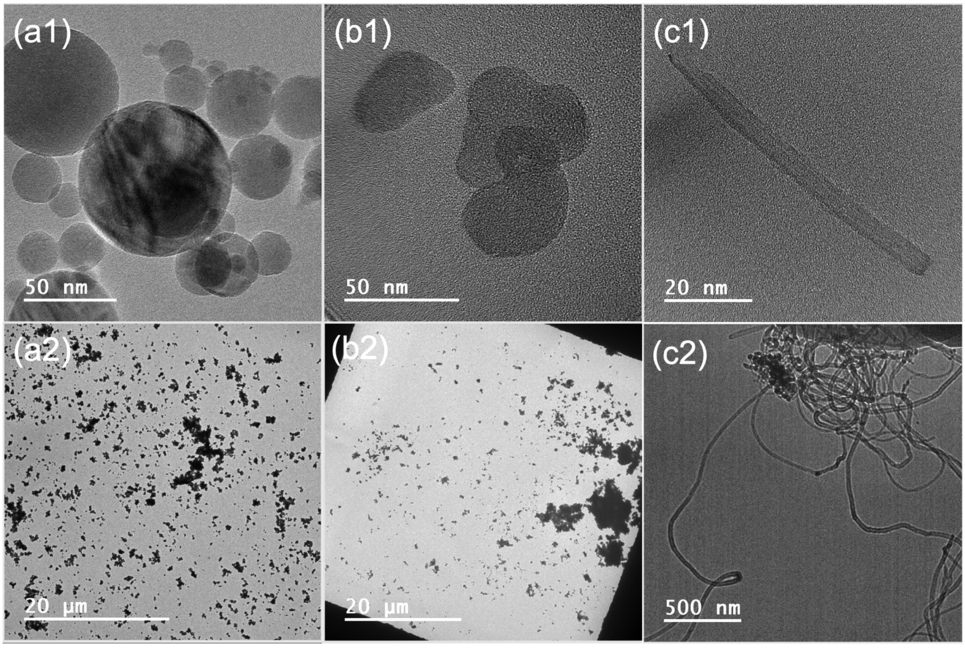

Figure 6. TEM images of sampled ENPs on grid collected on TDS samples: (a1, a2) Al_2O_3 at 50 nm and 20 μm scale bars, (b1, b2) carbon black at 50 nm and 20 μm scale bars, and (c1,c2) CNT at 50 and 500 nm scale bars.

an open-face cassette for inhalable-sized particles was used, while the Al_2O_3 collection was conducted using a closed-face cassette. The highest amount of released ENPs was collected from the surface of cotton and polyester cotton fabrics for all types of ENPs, while the least amount of ENPs was collected from the surface of polypropylene and Tyvek fabrics.

It seems clear that cotton fabric released the highest amount of carbon black ENPs based on the release mass concentration of total carbon with the value of 27 $\mu g/m^3$ or 20 μg/sample, while the least released fabric was polypropylene with the total carbon mass concentration of 16 $\mu g/m^3$. The released total carbon of Tyvek and polyester cotton fabric from the exposure of carbon black were 19 and 16 μg/sample, respectively. Based on the CNT ENP released total carbon results, cotton fabric was also found to be the most released fabric with the total carbon of 23 $\mu g/m^3$ and Tyvek fabric was observed with the lowest released of 17 $\mu g/m^3$. The current recommended exposure limit set by US NIOSH for CNTs is 1 $\mu g/m^3$ of total carbon.

The evidence of nanometer-sized particles resuspended from was further characterized using TEM and SEM, as shown in Figure 6. Individual particles and agglomerates of airborne Al_2O_3, carbon black, and CNT fibers released from the surface of the fabric are clearly seen in Figure 6.

Theoretical Discussion of Particle−Fabric Adhesion. The released number concentration of ENPs is ultimately determined by the strength of the nanoparticle adhesion to each fabric. A detailed accounting of the interaction between an ENP and a fabric surface is complicated because it depends upon many variables, most of which are unknown and difficult to accurately determine. For this reason, rather than focusing on numerical predictions for adhesion forces, we look for trends that can be inferred from the measurement of ENP release. A further complication is that a number of different physical forces can contribute to adhesion. While electrostatic charging may attract an ENP to a fabric, once in contact, other forces usually control how strongly an ENP adheres to the fabric. These forces can depend on the elemental chemical composition of both the ENP and fabric as well the separation distance between an ENP and the fabric. In the case of uncharged ENPs that do not chemically bond to a fabric surface, the dominant particle−substrate interaction is usually attributed to either (1) a surface force that arises from intermolecular van der Waals (vdW) interactions or (2) a capillary force due to a thin water bridge that forms between the ENP and the fabric surface. The influence of any electrostatic forces due to electrostatic charging is expected to dominate only when the ENP is separated from the substrate by a distance of ∼10 nm or more.

The integral form of the vdW molecular interaction (often called the Hamaker force) is typically larger than electrostatic forces and thus is often invoked as the dominant force that attracts nanometer-sized particles toward a surface. Once in contact, the force that holds the two bodies together is termed an adhesive force. If the interaction between the ENP and fabric is perfectly elastic, so no energy is dissipated during their interaction, and if no chemical reaction occurs, then the adhesive force will be equal in magnitude to the vdW surface force. The theoretical forces related to particle−fabric adhesion are described with details in the SI; the estimated Hamaker constants are presented in Table 2.

With estimates for H_{12}, checks can be made to determine if vdW interactions alone can qualitatively account for the trends observed for the release of ENPs presented in Figure 4. For example, if vdW interactions largely determine the adhesion of Al_2O_3 ENPs to the fabrics studied, then from the estimates of H_{12} in Table 2b, we see that to a first approximation, all H_{12} are about the same, i.e., $H_{12}^{\text{polyester−cotton}} \approx H_{12}^{\text{polypropolyene}} \approx H_{12}^{\text{polyethylene}} \approx H_{12}^{\text{cotton}}$. Thus, if the vdW interaction is the dominant adhesive force, all of the Al_2O_3 ENP release distributions from the various fabrics should have roughly the same shapes and magnitudes, especially for smaller values of the ENP diameter D_s. However, the measurements in Figure 4 showed that cotton preferentially released a significantly

https://doi.org/10.1021/acsanm.1c04229
ACS Appl. Nano Mater. 2022, 5, 2558−2568

Table 2. (a) Hamaker Constants for the Materials Used in This Study. (b) Estimates for the Interaction Hamaker Constants H_{12} Calculated Using Eq 2[a]

(a) Hamaker constants for materials of interest

	ENP or fabric	equivalent material	value (in J)
H_{11}	Al_2O_3	alumina	15.0×10^{-20}
	carbon black	carbon	47.0×10^{-20}
H_{22}	cotton	cellulose	5.8×10^{-20}
	polypropylene	polypropylene	6.0×10^{-20}
	Tyvek	HD polyethylene	6.3×10^{-20}
	polyester cotton	poly(ethylene terephthalate)	8.8×10^{-20}

(b) H_{12} (in J), from eq 2

	Al_2O_3	carbon black
cotton	9.3×10^{-20}	16.5×10^{-20}
polypropylene	9.5×10^{-20}	16.8×10^{-20}
Tyvek	9.7×10^{-20}	17.2×10^{-20}
polyester cotton	11.5×10^{-20}	20.3×10^{-20}

[a]Note: H_{12} is the Hamaker constant describing the interaction between the ENP 1 and the planar surface 2. H_{11} and H_{22} describe the interaction between a material 1 (or 2) with itself.

higher concentration of Al_2O_3 ENPs, implying that the vdW interaction for Al_2O_3 ENPs and cotton should be the weakest. This contradicts the predictions made on the basis of Table 2b, where all of the H_{12} have similar values.

A similar conclusion can be drawn by considering CB ENPs. As seen from Table 2b, the Hamaker constant H_{12} describing the interaction of CB ENPs with each fabric is ~1.8 times larger than for Al_2O_3. This implies that if vdW forces are dominant, the vdW adhesion force for a CB ENP to a fabric fiber should be about 1.8 times greater than that of an Al_2O_3 ENP of the same size. This would then further imply that the released number concentration of CB ENPs after shaking should be reduced by a factor of roughly 1/1.8 = 0.6 when compared to the released distribution of Al_2O_3 ENPs. Since the initial contamination distributions of CB and Al_2O_3 are very similar (see Figure 2), if vdW forces are dominant, the release concentration of CB ENPs should be roughly 0.6 the number concentrations measured for Al_2O_3 ENPs. Figure 3 indicates that while this expectation is approximately true for CB on cotton and polyester cotton, the expectation is not met for CB on Tyvek or polypropylene.

Taken together, an analysis of the systematics between the measured number concentrations of released Al_2O_3 and CB ENPs does not support the hypothesis that vdW forces constitute the dominant adhesive force for the various combinations of ENP/fabrics studied. A similar analysis for CNT ENPs was not attempted because the long tubular shape of the tangled CNTs is not well approximated by the sphere/plane geometry as required in Eq 1 above.

After ruling out vdW forces as the dominant adhesion force, the next interaction between an ENP and a fabric fiber we consider is capillarity. This interaction is related to the formation of a small bridge of moisture between an ENP and the fabric that supports it. A thin equilibrated water layer that depends on the relative humidity (RH) is present on all surfaces exposed to ambient conditions, and this thin water layer aids the water bridge formation. The RH in the lab then control the amount of water that will spontaneously condense in the small volume near the contact region between the ENP and the fabric surface. The water bridge serves to bind the ENP to the surface. In the limit of high humidity, complete immobilization of ENPs often result.

In the case of very low humidity, or if the surface chemistry of either the ENP or the fabric acts to prevent water condensation, the capillary force will be greatly reduced. Since cotton absorbs water, while polyester, polypropylene, and polyethylene do not, an ENP resting on a cotton fiber should show a reduction in the capillary force when compared to the other three fabric surfaces. This observation would in turn predict a significantly weaker adhesion of ENPs to cotton, resulting in a greater release of these ENPs when compared to the three other fabrics. This trend is, in fact, observed for Al_2O_3, CB, and CNT ENPs in Figure 4, a result that strongly suggests that capillarity likely plays a dominant role in affixing ENPs to the fabrics under study.

A secondary trend can be discerned by examining the ENP release data from polyester cotton fabric in Figure 3. The measured released number concentrations from polyester cotton are somewhat larger than the release distributions from polyethylene and polypropylene. The implication is that the 20% cotton fibers present in the polyester cotton blend fabric play a role in ENP adhesion. It is likely that the 20% cotton fibers interwoven between the 80% majority of polyester fibers enhance the wicking of condensed moisture, thereby reducing the effects of capillary forces between ENPs and the polyester cotton fabric surface.

Mechanical Properties (Durability) of Lab Coat Fabrics. Figure S3 shows representative strain−stress curves of the four untreated fabrics including cotton woven, polyester cotton woven, Tyvek nonwoven, and polypropylene nonwoven. The stress−strain curves of cotton and polyester cotton woven were similar, while those of Tyvek and polypropylene nonwoven were similar. The curves of two woven fabrics can be divided into two zones at the yield point: the first zone corresponds to the situation when the yarns within the fabrics move due to friction, resulting in deformation of weaves; the second zone is associated with the elongation of the yarns until the yarns break at the point of breaking shown on the strain−stress curves. Higher tensile strength was found in the polyester cotton (39.74 ± 6.50 MPa) than in the cotton (30.39 ± 4.00 MPa), suggesting that the polyester cotton fabric is stronger than the cotton fabric. The addition of polyester yarns to cotton enables reinforcement of cotton fabric. The polyester cotton Young's modulus (97.85 ± 10.00 MPa) is lower than the Young's modulus of cotton (152.15 ± 10.00 MPa).

On the other hand, the two nonwoven fabrics (Tyvek and polypropylene) showed significantly different behaviors when they were stretched in comparison with the woven fabrics. They were stretchy without true breaking during the test. Tyvek fabric demonstrated immediate plastic deformation, and the stress flattens at approximately 0.5% strain. Polypropylene fabric showed plastic deformation during the entire test. The tensile strengths of the Tyvek and polypropylene fabrics were 11.64 ± 3.35 and 3.11 ± 0.81 MPa, respectively. Although they were notably lower than those of cotton and polyester cotton fabrics, the Tyvek still showed a considerable strength against stretching compared to polypropylene. No Young's modulus was reported for the nonwoven fabrics, suggesting that both nonwoven fabrics are soft.

In summary, the cotton and polyester cotton woven have high strength and stiffness and hence would have substantial durability in the workplace when compared to the Tyvek and

https://doi.org/10.1021/acsanm.1c04229
ACS Appl. Nano Mater. 2022, 5, 2558−2568

polypropylene lab coats. Comparing Tyvek to polypropylene, Tyvek showed appreciable durability when being used in lab coats.

Abrasion resistance is the ability of a fabric to resist surface wear caused by flat rubbing and can also be used to measure fabric durability. Table S6 shows abrasion resistance measuring the average cycle before fabric failure that was defined by onsite of visible holes on fabric surface. The woven fabrics showed significantly higher abrasion resistance than the nonwoven fabrics. In addition, cotton was nearly twice as strong as polyester cotton against rubbing. First, the cotton fabric was thicker than the polyester cotton. Second, it was because the cotton woven has a twill structure that has more interlacing than a plain weave. Therefore, twill woven hold yarns together more efficiently than plain woven. The Tyvek and polypropylene coats both have substantially low abrasion resistance. The results were in a good agreement with the strain−stress curve results, suggesting that the cotton and polyester cotton fabrics have superior mechanical properties, while the Tyvek and polypropylene fabrics are weak materials and would be used to make disposable lab coats.

Water contact angle (WCA) analysis of the four fabrics are shown in Table S7. These data revealed that the Tyvek and polypropylene coats are hydrophobic (with static WCA of 125.9 ± 4.5 and 121.7± 6.3°, respectively) and the cotton polyester and cotton coats are hydrophilic (absorption rates of 4.24 ± 0.75 and 18.9 ± 3.5 μL/s, respectively). From the known chemical structures and X-ray photoelectron spectroscopy (XPS) analysis, these results are expected as polypropylene and Tyvek (patented type of high-density polyethylene) are synthetic fibers composed of hydrocarbon polymers, while the woven materials contain some oxygen functionality.

CONCLUSIONS

This study showed substantial particle release results for all types of tested fabrics. The release concentration for cotton and polyester cotton fabric was determined to be the highest from the aerosolization of Al_2O_3 and carbon black ENPs, while Tyvek and polypropylene showed the lowest amount of release concentration. From the exposure of CNT ENPs, the cotton fabric showed the highest release concentration compared with other tested fabrics. The release concentrations of cotton and polyester cotton were significantly different from Tyvek and polypropylene for Al_2O_3 and carbon black ENPs, while for CNT ENPs, cotton fabric turned out to be significantly different from all other fabric. Moreover, for all types of tested fabrics, the total number concentrations of resuspended ENPs at the breathing zone are higher than particles released from the back side of the worker wearing the contaminated protective clothing. Regarding exposure to multiple ENPs, it will require further studies to discover the rules of contamination based on chemical composition, particle size, and other surface properties of a mixture.

The total number concentration from 1 h contamination and 6 h release processes could represent the exposure of full-shift work presenting the risk of human exposure. Based on results of mass change measured before contamination and after the release processes, Tyvek fabric indicated the statistically highest value of mass change per unit mass from the exposure of Al_2O_3 and carbon black; for CNT ENPs, all fabrics showed a statistically similar level of mass change per unit mass. Some of the ENPs stay on the surface of the fabric due to the ENP adhesive forces. Two fundamental forces might be responsible for Al_2O_3 and carbon black ENP adhesion are van der Waals (vdW) force and capillary force, but it was difficult to determine for CNT ENPs due to their noncircular shape. Our analysis presented the dominant force for adhesion of ENPs with fabric fiber varies by environmental conditions (such as humidity). Capillary force can differ greatly with fabric absorbing moisture. A further study is ongoing investigating the mechanisms of adhesion and surface interactions between ENPs and fabric surface.

Overall, Tyvek is the best fabric for trapping all three types of studied ENPs, which eliminates the resuspension to expose humans. However, this fabric was not durable enough for workers to wear for the long term or the active motions at work might cause wear or tearing of the Tyvek fabric, reducing its barrier properties and enabling penetration of ENPs. The polypropylene fabric is the next most effective for trapping ENPs of all three types. In addition, three types of ENPs were found to cause some difference in terms of adhesion onto the fabric surface, and we found that the Al_2O_3 ENPs remained on the fabric the most, especially more on the Tyvek fabric, after simulated working activities, compared to other carbon black and CNT ENPs. Cotton and polyester cotton lab coats were found to be the least effective fabric type for trapping ENPs. Although these fabrics are the most durable, comfortable, and commonly used in workplaces, they are not recommended to be used when ENPs are present in work environments.

ASSOCIATED CONTENT

Supporting Information

The Supporting Information is available free of charge at https://pubs.acs.org/doi/10.1021/acsanm.1c04229.

Methods regarding fabric descriptive property measurements and airborne particle sampling using filter-based standard methods; aerosolization of ENPs for protective clothing contamination results, fabric descriptive property results, and the discussion of theoretical forces related to particle−fabric adhesion; statistical analysis results with comparisons of total number concentrations, particle size distributions, mass change, and ANOVA one way test on release total number concentration of Al_2O_3, carbon black, and CNT ENPs tables and figure (PDF)

AUTHOR INFORMATION

Corresponding Author

Candace Su-Jung Tsai − *Department of Chemical and Biological Engineering, Walter Scott, Jr. College of Engineering, Colorado State University, Fort Collins, Colorado 80523, United States; School of Advanced Materials Discovery and Department of Environmental and Radiological Health Sciences, College of Veterinary Medicine & Biomedical Sciences, Colorado State University, Fort Collins, Colorado 80523, United States; Department of Environmental Health Sciences, Fielding School of Public Health, University of California, Los Angeles, California 90095, United States;* orcid.org/0000-0002-7296-8278; Email: candacetsai@ucla.edu

Authors

Aigerim Maksot − *Department of Chemical and Biological Engineering, Walter Scott, Jr. College of Engineering,*

https://doi.org/10.1021/acsanm.1c04229
ACS Appl. Nano Mater. 2022, 5, 2558−2568

Colorado State University, Fort Collins, Colorado 80523, United States

Sadia Momtaz Sorna − *School of Advanced Materials Discovery, Colorado State University, Fort Collins, Colorado 80523, United States*

Melissa Blevens − *Department of Environmental and Radiological Health Sciences, College of Veterinary Medicine & Biomedical Sciences, Colorado State University, Fort Collins, Colorado 80523, United States*

Ronald G. Reifenberger − *Department of Physics, Purdue University, West Lafayette, Indiana 47907, United States*

Kimberly Hiyoto − *Department of Chemistry, Colorado State University, Fort Collins, Colorado 80523, United States*

Ellen R. Fisher − *Department of Chemistry, Colorado State University, Fort Collins, Colorado 80523, United States;* orcid.org/0000-0001-6828-8600

Tony Vindell − *School of Advanced Materials Discovery, Colorado State University, Fort Collins, Colorado 80523, United States*

Yan Vivian Li − *School of Advanced Materials Discovery and Department of Design and Merchandising, Colorado State University, Fort Collins, Colorado 80523, United States;* orcid.org/0000-0001-8009-9773

Matt J. Kipper − *Department of Chemical and Biological Engineering, Walter Scott, Jr. College of Engineering, Colorado State University, Fort Collins, Colorado 80523, United States; School of Advanced Materials Discovery, Colorado State University, Fort Collins, Colorado 80523, United States;* orcid.org/0000-0002-8818-745X

Complete contact information is available at: https://pubs.acs.org/10.1021/acsanm.1c04229

Author Contributions

The manuscript was written through the contributions of all authors.

Funding

This research was funded by the Department of Health and Human Services, Center for Disease Control and Prevention, Grant No. 1 R21OH011507-01.

Notes

The authors declare no competing financial interest.

■ ACKNOWLEDGMENTS

The authors would like to thank Dr. Roy Geiss and Rebecca Miller for technical support in TEM analysis, Rebecca Miller for support in SEM analysis.

■ ABBREVIATIONS

ENP, engineered nanoparticles
CB, carbon black
CNT, carbon nanotubes
NIOSH, National Institute for Occupational Safety and Health
vdW, van der Waals
AFM, atomic force microscope
SEM, scanning electron microscopy
TEM, transmission electron microscopy
PVC, poly(vinyl chloride)
MCE, mixed cellulose ester
NMAM, NIOSH Manual of Analytical Method
WCA, water contact angle
XPS, X-ray photoelectron spectroscopy

■ REFERENCES

(1) GlobalNanotechnology Market Outlook 2024 - Research and Markets. https://www.researchandmarkets.com/reports/4991720/global-nanotechnology-market-outlook-2024 (accessed January 17, 2021).
(2) Clemente, A.; Jiménez, R.; Encabo, M. M.; Lobera, M. P.; Balas, F.; Santamaria, J. Fast and Simple Assessment of Surface Contamination in Operations Involving Nanomaterials. *J. Hazard. Mater.* **2019**, *363*, 358−365.
(3) McDonagh, A.; Byrne, M. A. The Influence of Human Physical Activity and Contaminated Clothing Type on Particle Resuspension. *J. Environ. Radioact.* **2014**, *127*, 119−126.
(4) McDonagh, A.; Byrne, M. A. A Study of the Size Distribution of Aerosol Particles Resuspended from Clothing Surfaces. *J. Aerosol Sci.* **2014**, *75*, 94−103.
(5) Tsai, C. S. J. Contamination and Release of Nanomaterials Associated with the Use of Personal Protective Clothing. *Ann. Occup. Hyg.* **2015**, *59*, 491−503.
(6) Licina, D.; Nazaroff, W. W. Clothing as a Transport Vector for Airborne Particles: Chamber Study. *Indoor Air* **2018**, *28*, 404−414.
(7) Liang, X.; Xu, Z.; Grice, J.; Zvyagin, A.; Roberts, M.; Liu, X. Penetration of Nanoparticles into Human Skin. *Curr. Pharm. Des.* **2013**, *19*, 6353−6366.
(8) NIOSH, Manual of Analytical Methods (NMAM) 4th ed.
(9) ASBESTOS by TEM 7402, 1989.
(10) CDC; Niosh NMAM0500: PARTICULATES NOT OTHERWISE REGULATED, TOTAL.
(11) Tsai, C. S. J.; Theisen, D. A Sampler Designed for Nanoparticles and Respirable Particles with Direct Analysis Feature. *J. Nanopart. Res.* **2018**, *20*, No. 209.
(12) Thayer, D.; Koehler, K. A.; Marchese, A.; Volckens, J. A Personal, Thermophoretic Sampler for Airborne Nanoparticles. *Aerosol Sci. Technol.* **2011**, *45*, 744−750.
(13) Leith, D.; Miller-Lionberg, D.; Casuccio, G.; Lersch, T.; Lentz, H.; Marchese, A.; Volckens, J. Development of a Transfer Function for a Personal, Thermophoretic Nanoparticle Sampler. *Aerosol Sci. Technol.* **2014**, *48*, 81−89.
(14) Tsai, S. C.; Ada, E.; Isaacs, J. A.; Ellenbecker, M. J. Airborne Nanoparticle Exposures Associated with the Manual Handling of Nanoalumina and Nanosilver in Fume Hoods. *J. Nanopart. Res.* **2009**, *11*, 147−161.
(15) Old, L.; Methner, M. M. Effectiveness of Local Exhaust Ventilation (LEV) in Controlling Engineered Nanomaterial Emissions during Reactor Cleanout Operations. *J. Occup. Environ. Hyg.* **2008**, *5*, D63−D69.
(16) Methner, M.; Hodson, L.; Dames, A.; Geraci, C. Nanoparticle Emission Assessment Technique (NEAT) for the Identification and Measurement of Potential Inhalation Exposure to Engineered Nanomaterials—Part b: Results from 12 Field Studies. *J. Occup. Environ. Hyg.* **2010**, *7*, 163−176.
(17) Hämeri, K.; Lahde, T.; Hussein, T.; Koivisto, J.; Savolainen, K. Facing the Key Workplace Challenge: Assessing and Preventing Exposure to Nanoparticles at Source. *Inhalation Toxicol.* **2009**, *21*, 17−24.
(18) Park, J.; Kwak, B. K.; Bae, E.; Lee, J.; Kim, Y.; Choi, K.; Yi, J. Characterization of Exposure to Silver Nanoparticles in a Manufacturing Facility. *J. Nanopart. Res.* **2009**, *11*, 1705−1712.
(19) Miller, A.; Drake, P. L.; Hintz, P.; Habjan, M. Characterizing Exposures to Airborne Metals and Nanoparticle Emissions in a Refinery. *Ann. Occup. Hyg.* **2010**, *54*, 504−513.